Pattern Diversity with Multi-mode Circular Patch Antennas in Clustered MIMO Channels

Antonio Forenza*, Frank Sun, and Robert W. Heath Jr.
WNCG, ECE Department, The University of Texas at Austin, TX, USA
{forenza,wsun,rheath}@ece.utexas.edu

I. INTRODUCTION

The throughput that a MIMO channel can support is a function of different array parameters such as element spacing, number of antennas and array geometry [1], [2]. Although there is significant prior work, the emphasis is on spaced array configurations. In typical MIMO systems, the size constraints often prevents the antennas from being placed far apart (e.g., antenna placement in notebook computers or mobile phones). Therefore, spatial diversity technique may not provide the complete solution for next generation wireless handsets.

An alternative technique for miniaturized antenna designs is polarization/pattern diversity [3]–[6], where the antennas are designed to radiate with orthogonal radiation patterns and polarizations as a means to create uncorrelated channels across different array elements. The benefits of pattern diversity have been shown in [6]. That analysis however did not use realistic channel models.

In this contribution we aim to extend the analysis in [6] to clustered channel models, adopted by the IEEE 802.11n standard body for wireless local area networks (WLANs). We analyze MIMO arrays consisting of circular microstrip antennas to enable pattern diversity and compare their performance against conventional uniform linear arrays. We will also model the effect of mutual coupling as in [7] and measure the performance degradation produced by the near-field effects. Hereafter, we briefly review the channel model and the properties of circular microstrip antennas. Then, we analytically compute the spatial correlation coefficients and evaluate the MIMO channel capacity.

II. CHANNEL AND SYSTEM MODELS

We simulate the MIMO channel according to the clustered channel model proposed by IEEE 802.11n, described in [8]. For simulation purposes, we discard the line-of-sight component of the channel and generate each matrix tap according to the correlated Rayleigh fading model as

$$\mathbf{H} = \mathbf{R}_r^{1/2}\mathbf{H}_w\mathbf{R}_t^{T/2} \tag{1}$$

where $\mathbf{H}_w \in \mathbb{C}^{N_r \times N_t}$ is a matrix of complex Gaussian fading coefficients, while $\mathbf{R}_t$ and $\mathbf{R}_r$ denote the transmit and receive spatial correlation matrices, respectively. The entries of the spatial correlation matrices are derived in closed form accounting for the antenna radiation patterns and the spatial characteristics of the clusters, as described in the next section.

The properties of circular microstrip antennas have been extensively studied in [9], [10]. In [9] it was shown that, by exciting different modes of circular patch antennas, it is possible to obtain different radiation properties. Moreover, by varying the size of the antennas as well as the feeding points, different polarizations and radiation patterns can be generated in far-field. In this paper we exploit the orthogonality of the radiation patterns of circular patch antennas as a means to obtain significant diversity gains.

We express the electric field of n-th mode excited in the circular patch as a function of its θ and ϕ far-field components, that can be written as [9]

$$E_\theta^{(n)} = e^{jn\pi/2}\frac{V_0^{(n)}}{2}k_0\rho\,(J_{n+1} - J_{n-1})\cos n(\phi - \phi_0) \tag{2}$$

$$E_\phi^{(n)} = -e^{jn\pi/2}\frac{V_0^{(n)}}{2}k_0\rho\,(J_{n+1} + J_{n-1})\cos\theta\sin n(\phi - \phi_0) \tag{3}$$

where V_0 is the input voltage, k_0 is the wavenumber, $J_n = J_n(k_0\rho\sin\theta)$ is the Bessel function of the second kind and order n, ρ is the radius of the microstrip antenna and ϕ_0 is the angle corresponding to the feeding point of the antenna. Depending on the mode excited inside the patches of the MIMO array, we tune the phase ϕ_0 to produce orthogonal radiation patterns across the diversity branches. Moreover, we assume the patch antennas to be collocated and stacked on top of each other, as described in [9], to isolate the effect of pattern from space diversity.

0-7803-8883-6/05/$20.00 ©2005 IEEE

III. Spatial Correlation Coefficients

We model the signal received at the i-th antenna of the MIMO array as [5]

$$y_i = \int_{\Delta\Omega} \underline{e}_i(\Omega) \cdot \underline{E}_i(\Omega) d\Omega \tag{4}$$

where $\Omega = (\phi, \theta)$ is the solid angle, $\Delta\Omega$ is the source region, $\underline{E}_i(\Omega) = E_{i,\theta}\widehat{\theta} + E_{i,\phi}\widehat{\phi}$ is the far-field of the circular patch with θ and ϕ components given in equations (2) and (3), $\underline{e}_i(\Omega)$ is the propagating filed that impinges the antenna from the angular direction Ω.

From equation (4) we derive the correlation coefficient across the i-th and k-th antennas of the MIMO array as

$$r_{ik} = \mathcal{E}\{y_i y_k^*\} = \int_{\Delta\Omega} S(\Omega) \underline{E}_i(\Omega) \underline{E}_k^*(\Omega) d\Omega \tag{5}$$

where $S(\Omega)$ is the power angular spectrum (PAS). We assume the PAS over the θ angles to be independent from the ϕ angles and we write $S(\Omega) = S(\theta)S(\phi)$. We generate the power azimuth spectrum $S(\phi)$ according to the truncated Laplacian distribution as in [8]. Since the elevation angle spread is generally smaller than the azimuth spread, we assume $S(\theta) = \delta(\theta - \pi/2)$ to simplify our analysis.

We now consider two circular patch antennas, both excited with the n-th mode, with feeding angles $\phi_0^{(1)} = 0$ and $\phi_0^{(2)} = \pi/(2n)$ to produce orthogonal patterns. Under these assumptions, substituting equations (2) and (3) into (5), and accounting for the defined PAS, we write the autocorrelation coefficient for the first antenna as

$$r_{11} = |\alpha^{(n)}(\rho)|^2 \left[J_{n+1}(k_0\rho) - J_{n-1}(k_0\rho)\right]^2 \int_{\Delta\phi} S(\phi) \cos^2(n\phi) d\phi \tag{6}$$

where $\alpha^{(n)}(\rho) = e^{jn\pi/2}(V_0^{(n)}/2)k_0\rho$. Solving the integral in (6) we derive

$$\begin{aligned} r_{11}(\phi_c, \sigma_\phi) &= \tfrac{|\alpha^{(n)}(\rho)|^2 (n\sigma_\phi)^2}{1+2(n\sigma_\phi)^2} \left[J_{n+1}(k_0\rho) - J_{n-1}(k_0\rho)\right]^2 \\ &\quad \cdot \left[1 - e^{-\sqrt{2}\pi/\sigma_\phi} + \tfrac{\cos^2(n\phi_c)}{(n\sigma_\phi)^2}\left(1 - e^{-\sqrt{2}\pi/\sigma_\phi}\cos^2(n\pi)\right)\right] \end{aligned} \tag{7}$$

where ϕ_c and σ_ϕ are the mean angle of arrival and angle spread of the cluster over the azimuth plane, respectively. The autocorrelation coefficient for the second patch is derived from equation (7), accounting for the angle shift ($\phi_0^{(2)}$) across the two antennas, and $r_{22}(\phi_c, \sigma_\phi) = r_{11}(\phi_c - \phi_0^{(2)}, \sigma_\phi)$.

To derive the cross-correlation coefficients we start from equation (5) and derive

$$r_{12} = \frac{|\alpha^{(n)}(\rho)|^2}{2} \left[J_{n+1}(k_0\rho) - J_{n-1}(k_0\rho)\right]^2 \int_{\Delta\phi} S(\phi) \sin(2n\phi) d\phi. \tag{8}$$

Solving the integral in (8) we get

$$r_{12}(\phi_c, \sigma_\phi) = \frac{|\alpha^{(n)}(\rho)|^2}{1 + 2(n\sigma_\phi)^2} \left[J_{n+1}(k_0\rho) - J_{n-1}(k_0\rho)\right]^2 \cdot \left(1 - e^{-\sqrt{2}\pi/\sigma_\phi}\right) \sin(2n\phi_c). \tag{9}$$

Note that the cross-correlation coefficient r_{21} has the same expression as equation (9).

IV. Results on Pattern Diversity

In this section we compare the performance of a 2-element circular patch array (CPA) versus 2-element uniform linear array (ULA) in a single-cluster MIMO channel. The CPA consists of two collocated circular patch antennas, with same mode number and orthogonal radiation patterns. The ULA is designed with 2 vertically polarized half-wavelength dipoles, with variable element spacing. We investigate the possible benefits of pattern diversity (for the CPA) and space diversity (for the ULA) over the performance of MIMO systems in different propagation scenarios.

In Fig. 1 we report the correlation coefficients for the CPA, excited with mode 2. We simulated a single cluster with a variable mean angle of arrival (ϕ_c) and angle spread $\sigma_\phi = 20^o$ over the azimuth plane. The "empirical" correlation coefficients are obtained through MATLAB simulations, carried out with 5000 rays distributed according to the PAS aforementioned. The "theoretical" coefficients are computed through equations (7) and (9). Fig. 1 shows that the closed-form of the correlation coefficients derived analytically reproduces exactly the coefficients derived empirically. This result

makes the equations (7) and (9) a useful tool to analyze the performance of the CPA, as described in the following paragraphs.

In Fig. 2 we compare the envelop correlation coefficients of the CPA (with mode 3) against the ULA (with element spacing of $\lambda/2$), for single cluster with $\sigma_\phi = 15^o$. We generate the correlation coefficients of the ULA through the closed-form expression derived in [11], for Laplacian distributed angles of arrival. The oscillations of the envelop correlation of the CPA are due to the multiple lobes in the radiation patterns of the patch antennas. For the ULA, the autocorrelation is always 1, whereas the cross-correlation coefficients are a function of ϕ_c. In the same plot we depict the MIMO channel capacity at $SNR = 5$dB for the two arrays, assuming spatial correlation only at the transmit side. We computed the ergodic capacity employing the tight upper bound for zero mean spatially correlated MIMO channels derived in [12]. The capacity of the CPA has small oscillations around its mean value, which are not visible in Fig. 2. The capacity of the ULA reaches its maximum and minimum values at broadside and endfire directions, respectively, as already acknowledged in [2]. Interestingly, the CPA with mode 3 outperforms the ULA for any direction of arrival.

In Fig. 3 we report the MIMO channel capacity at $SNR = 5$dB for the ULA and the CPA with different modes, in single-cluster channel with $\sigma_\phi = 30^o$. For mode 1 the CPA outperforms the ULA only for angles close to endfire directions. In fact, the radiation pattern of mode 1 consists of only 2 lobes over the azimuth directions, which makes pattern diversity less effective than space diversity. For any other mode, the CPA always provides better performance than the ULA due to the increasing number of lobes in the radiation pattern of the higher modes. This result shows the benefit of pattern over space diversity in single-cluster channels.

Finally, Fig. 4 depicts the average MIMO channel capacity (with correlation only at the receive side), accounting for mutual coupling, as a function of the SNR. We measured the effects of mutual coupling for the ULA and CPA through FEKO, an EM software tool based on the method of moments. Then, we used the model for mutually-coupled antennas described in [7] to derive the MIMO capacity through Montecarlo simulations. We designed the antennas to operate at the carrier frequency of 2.45GHz. For the CPA we excited the mode 3 with $\epsilon_r = 2.5$, physical radius $\rho = 0.41\lambda$, feeding point $\rho_0 = 0.8\rho$, height of the patch $h = 1.575$mm. The first set of curves is referred to the ULA with element spacing $\lambda/2$ (i.e., ULA1) and low angle spread (i.e., $\sigma_\phi = 15^o$). In this channel condition, the CPA yields 0.8dB and 1.8dB gains at $SNR = 10$dB over the ULA at broadside and endfire directions, respectively. Therefore, in this conditions, pattern diversity yields higher performance than space diversity, as expected. The second set of curves is obtained for the ULA with element spacing 2.5λ (i.e., ULA2), high angle spread (i.e., $\sigma_\phi = 40^o$) and cluster located at broadside direction of the ULA2. The MIMO capacity of the CPA is very close to the ULA2, while satisfying the limited size constraint. These results clearly show the benefit of pattern diversity versus space diversity with 2-element ULA and CPA, in single-cluster MIMO channels.

V. Conclusion and Future Work

We studied the performance of 2-element circular patch arrays (CPA) with collocated antennas, employing pattern diversity technique. We showed that pattern diversity yields better performance than space diversity, achieved with 2-element uniform linear arrays (ULA) with spacing $\lambda/2$, in single-cluster channels. The CPA performs similarly to the ULA with spacing of 2.5λ (i.e., 30cm at carrier frequency of 2.45GHz), while providing a more compact design. These results show the great potential of CPA for compact array designs for notebook computers or access points in WLANs. Future investigations include further miniaturization of the CPA design and performance study in typical channel models for indoor environments described in [8].

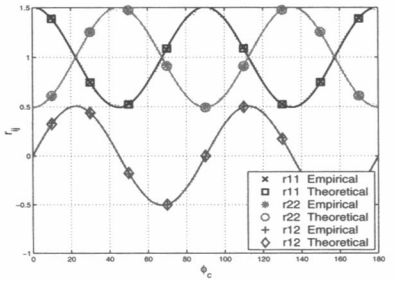

Fig. 1. Empirical and theoretical correlation coefficients for the CPA, with mode 2, $\sigma_\phi = 20^o$.

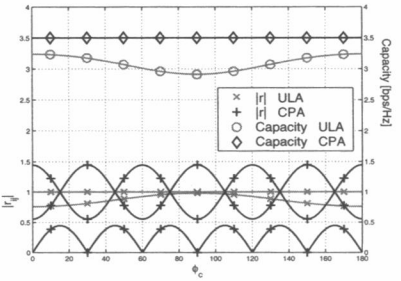

Fig. 2. Envelop correlation and mean capacity for the ULA and CPA, with mode 3, ULA spacing of $\lambda/2$, $\sigma_\phi = 15^o$, $SNR = 5$dB.

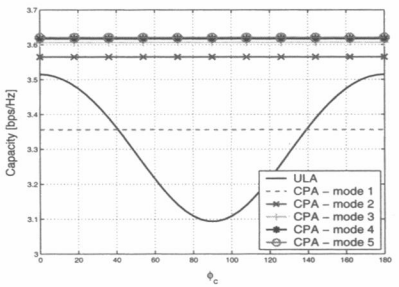

Fig. 3. Mean capacity for the ULA and CPA, with mode 3, ULA spacing of $\lambda/2$, $\sigma_\phi = 30^o$, $SNR = 5$dB.

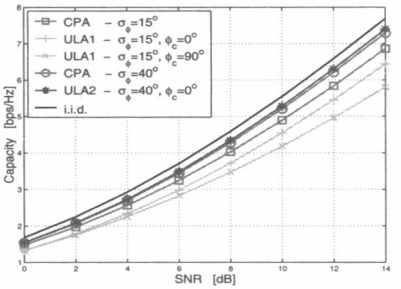

Fig. 4. Mean capacity of ULA and CPA, with mutual coupling effects, for mode 3, $\rho = 0.41\lambda$, spacing d(ULA1)= $\lambda/2$ and d(ULA2)= 2.5λ.

REFERENCES

[1] D.-S. Shiu, G. J. Foschini, M. J. Gans, and J. M. Kahn, "Fading correlation and its effect on the capacity of multielement antenna systems," *IEEE Trans. Commun.*, vol. 48, no. 3, pp. 502–513, Mar. 2000.

[2] A. Forenza and R. W. Heath Jr., "Impact of antenna geometry on MIMO communication in indoor clustered channels," *Proc. IEEE Antennas and Prop. Symp.*, vol. 2, pp. 1700 – 1703, June 2004.

[3] M. R. Andrews, P. P. Mitra, and R. deCarvalho, "Tripling the capacity of wireless communications using electromagnetic polarization," *Nature*, vol. 409, pp. 316–318, Jan. 2001.

[4] C. Waldschmidt, C. Kuhnert, S. Schulteis, and W. Wiesbeck, "Compact MIMO-arrays based on polarisation-diversity," *Proc. IEEE Antennas and Prop. Symp.*, vol. 2, pp. 499 – 502, June 2003.

[5] T. Svantesson, M. A. Jensen, and J. W. Wallace, "Analysis of electromagnetic field polarizations in multiantenna systems," *IEEE Trans. Wireless Comm.*, vol. 3, pp. 641 – 646, Mar. 2004.

[6] L. Dong, H. Choo, H. Ling, and Jr. R. W. Heath, "MIMO wireless handheld terminals using antenna pattern diversity," *to appear in IEEE Trans. on Wireless.*, Aug. 2003.

[7] M. L. Morris and M. A. Jensen, "Network model for MIMO systems with coupled antennas and noisy amplifiers," *IEEE Trans. Antennas Propagat.*, vol. 53, pp. 545 – 552, Jan. 2005.

[8] V. Erceg, L. Schumacher, P. Kyritsi, A. Molisch, D. S. Baum, A. Y. Gorokhov, C. Oestges, Q. Li, K. Yu, N. Tal, B. Dijkstra, A. Jagannatham, C. Lanzl, V. J. Rhodes, J. Medbo, D. Michelson, M. Webster, E. Jacobsen, D. Cheung, C. Prettie, M. Ho, S. Howard, B. Bjerke, L. Jengx, H. Sampath, S. Catreux, S. Valle, A. Poloni, A. Forenza, and R. W. Heath, "TGn channel models," *IEEE 802.11-03/940r4*, http://www.802wirelessworld.com:8802/, May 2004.

[9] R. G. Vaughan, "Two-port higher mode circular microstrip antennas," *IEEE Trans. Antennas Propagat.*, vol. 36, pp. 309 – 321, Mar. 1988.

[10] R. G. Vaughan and J. Bach Anderson, "Antenna diversity in mobile communications," *IEEE Trans. on Veh. Technol.*, vol. VT-36, pp. 149 – 172, Nov. 1987.

[11] L. Schumacher, K. I. Pedersen, and P.E. Mogensen, "From antenna spacings to theoretical capacities - guidelines for simulating MIMO systems," *Proc. IEEE Int. Symp. on Pers., Indoor and Mobile Radio Comm.*, vol. 2, pp. 587–592, Sep. 2002.

[12] H. Shin and J. H. Lee, "Capacity of multiple-antenna fading channels: spatial fading correlation, double scattering, and keyhole," *IEEE Trans. Info. Th.*, vol. 49, pp. 2636 – 2647, Oct. 2003.